JOURNAL OF MATERIALS SCIENCE 27 (1992) 6371–6378

Structure and mechanics of cement foams

T. D. TONYAN, L. J. GIBSON
Department of Civil Engineering, Massachusetts Institute of Technology, Cambridge, MA 02139, USA

Lightweight cellular concretes have been available for a number of years. They are made by adding aluminium powder to the cement mix or by introducing a foaming agent to a cement slurry. Materials with densities in the range 320–1600 kg m^{-3} are commonly available commercially; they are used for insulated concrete roof-deck systems, masonry blocks, cladding panels and engineered fills for geotechnical applications. Their unique set of properties make them attractive as a foam core material for structural sandwich panels: they have moderate thermal insulation, high heat capacity, high stiffness, excellent fire resistance and low cost relative to polymer foams. The structure and mechanical behaviour of cellular cements ranging in density from 160–1600 kg m^{-3} are described.

1. Introduction

Cement foams are used in an increasing number of applications. Cast-in-place cement foams are used for insulating roof-deck systems and for engineered fills for geotechnical applications, while precast autoclaved products are widely used as load-bearing blocks, reinforced wall, roof and floor units and as non-load-bearing cladding panels over a primary structural frame.

Cement foams can be made either by a chemical or a mechanical foaming process. In the chemical process, a finely powdered metal, usually aluminium, is added to a slurry composed of cement, lime and often a siliceous filler such as silica flour, pulverized fuel ash, ground burnt shale or blast furnace slag. The aluminium reacts with the lime in the slurry, producing hydrogen gas bubbles as indicated by the following equation

$$\underset{\text{aluminium powder}}{2Al} + \underset{\text{hydrated lime}}{3Ca(OH)_2 + 6H_2O} \Rightarrow \underset{\text{tricalcium aluminate hydrate}}{3CaO{*}Al_2O_3{*}6H_2O} + \underset{\text{hydrogen gas}}{3H_2} \quad (1)$$

The hydrogen gas is quickly replaced by air, eliminating the fire hazard. Most aerated concretes produced with this method have densities between 480 and 960 kg m^{-3}; densities as low as 240 kg m^{-3} have been produced [1, 2].

Mechanical foaming processes introduce a foaming agent into the cement slurry in one of two ways: the foaming agent can be added directly to the cement slurry which is then agitated to form a stable mass, or a preformed foam, made by pressurizing an aqueous solution of the foaming agent with compressed air, can be introduced into the cement slurry and mixed. The preformed foams typically provide better control of density and foam cell structure and are more suitable for making low-density foams. Several types of foaming agents are available for the production of cement foams, including saponified wood resin stabilized with animal glue, sodium compounds of aliphatic and aromatic sulphates (such as sodium lauryl, cetyl and oleyl sulphates and sodium napthalene isopropyl sulphate), sulphates of petroleum derivatives, complex organic compounds (such as keratin and saponin), and proprietary foaming agents [1].

In both the chemical and mechanical processes described above, the cement foam is usually cured in a moist environment at ambient temperatures. High-pressure steam curing in an autoclave improves the properties of cement foams: precastable autoclaved lightweight ceramic (PALC), cured for 8 h at 180 °C and 1 MPa pressure, is an example of an autoclaved cement foam product [3].

The microstructures of several densities of cement foams are shown in Fig. 1. For the 720 kg m^{-3} cement foam shown in Fig. 1a the individual cells range in diameter from 20–500 μm, with an average of roughly 200 μm. Note that as the density decreases, individual cells tend to coalesce, forming larger voids. At densities of less than 240 kg m^{-3}, the coalesced cells can be up to 3 mm diameter.

The compressive load–deflection curve for a foamed cement is shown in Fig. 2; it is typical of that of a cellular material. The material is linear elastic up to the peak stress, at which point the stress drops sharply and is then maintained at a plateau level up to large strains.

Data for the mechanical properties of cement foams at densities as low as 480 kg m^{-3} have been reported by Reichard [4] and Short and Kinniburgh [2]. Typical values for a 480 kg m^{-3} material are Young's modulus 460 MPa, compressive strength 0.69 MPa,

0022–2461

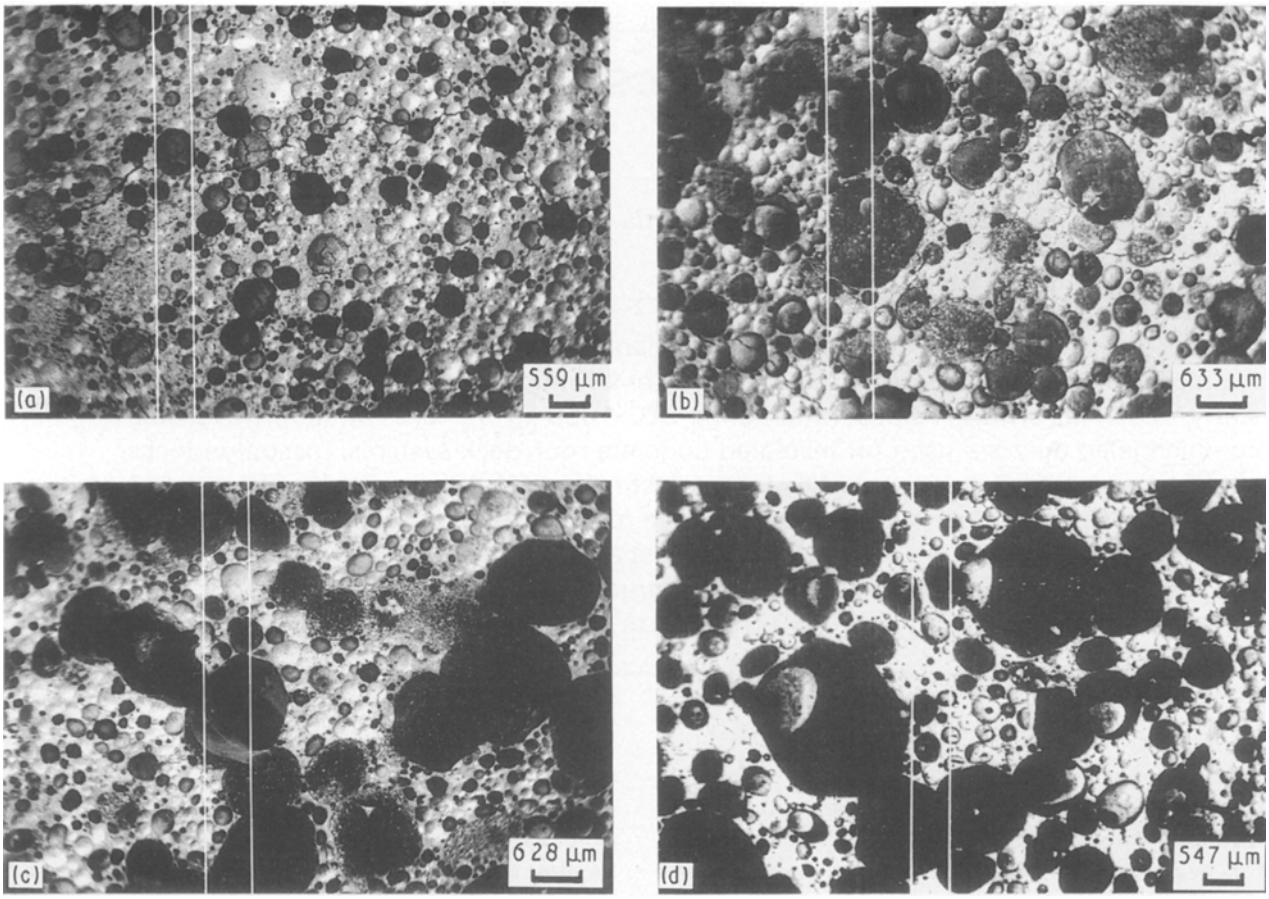

Figure 1 Scanning electon micrographs showing the structure of cement foams: (a) 720, (b) 400, (c) 320, and (d) 240 kg m^{-3}. Note that at 720 kg m^{-3} few of the voids have coalesced. As the density is reduced, the volume fraction of large, coalesced voids increases.

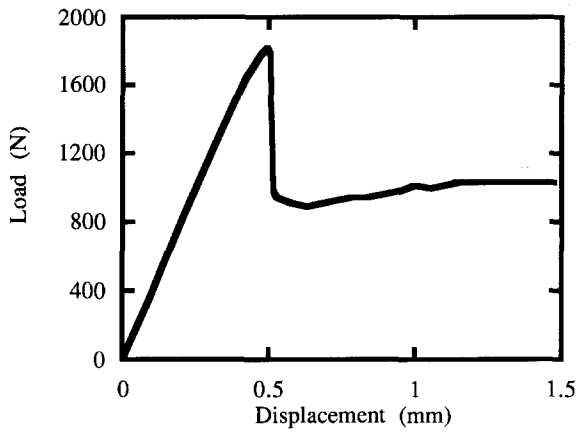

Figure 2 A load–deflection plot for a 350 kg m^{-3} cement foam cylinder tested in compression.

and modulus of rupture 0.24 MPa. Autoclaved material PALC, at the same density of 480 kg m^{-3}, has superior mechanical properties: its Young's modulus is 1725 MPa, its compressive strength is 4.1 MPa, and its tensile strength is 0.69 MPa. The thermal resistance, R, of cement foams and PALC are plotted against density in Fig. 3: at 240 kg m^{-3}, R increases to 80 °C W^{-1}, a value close to that of polystyrene foams currently used in building panels.

In this study we have characterized the microstructure and mechanical properties of non-autoclaved cement foams made using a preformed foam process. The results have been compared with models for the mechanical behaviour of cellular materials modified to take account of the unique microstructural features of cement foams.

2. Experimental methods

2.1. Processing of preformed cement foam

The cement foams tested in this study were made using a preformed foam process in which a simple cement and water slurry was combined with the preformed foam. The stability and properties of the foam were improved by the inclusion of various additives: a microsilica-based liquid admixture increased the cohesiveness of the cement foam during setting and reduced the permeability of the hardened cement paste; a superplasticizer reduced the water/cement ratio of the mix while maintaining a stable foam; and polyester fibres enhanced foam stability during setting and hardening and improved the tensile properties in the hardened cement foam. A sample mix design for a typical 320 kg m^{-3} cement foam is given in Table I [5].

The mixing process is shown in Fig. 4. The dry cement was first mixed with the polyester fibres in a large mixing bowl by hand. Water heated to 49 °C, silica fume solution and superplasticizer were then added to the cement and further mixed by hand. The foaming agent, a proprietary synthetic material (Elastizell Corporation of America, Ann Arbor, MI), was

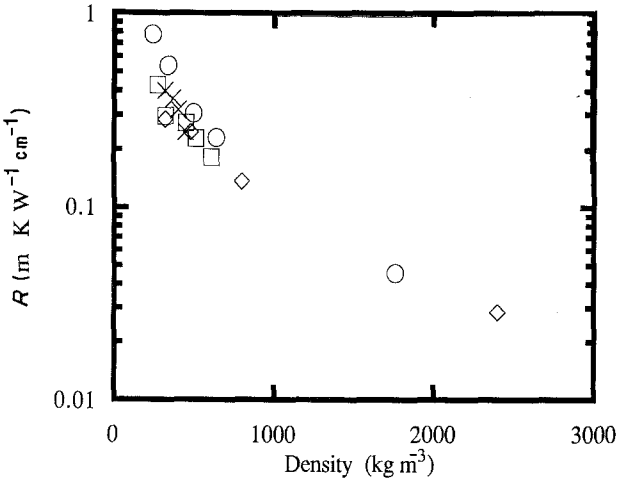

Figure 3 Thermal resistance of cement foams plotted against density. (○) Cement foam [1], (□) cement foam (Elastizell), (◇) ALC [2], (×) PALC [3].

TABLE I 320 kg m^{-3} mix design

Component	Weight (N)
Water (49 °C)	23.4
Cement[a]	44.5
Microsilica[b]	6.50
Polyester fibre (38 mm)[c]	0.15
Superplasticizer[d]	0.22
Preformed foam[e]	8.86 (0.02 m^3)

[a] Portland Cement Type III.
[b] Force 10,000, W. R. Grace, Cambridge, MA, USA.
[c] Zell-Crete Fibre, Elastizell Corporation of America, Ann Arbor, MI, USA.
[d] ZIP, Elastizell Corporation of America, Ann Arbor, MI, USA.
[e] EMG, Elastizell Corporation of America, Ann Arbor, MI, USA.

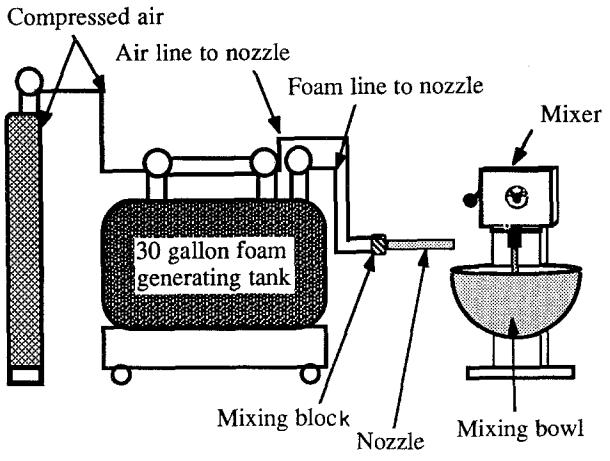

Figure 4 Schematic drawing showing the equipment used for processing the cement foams. 1 gallon = 4.546 l.

diluted in a 1:30 solution with water and pressurized in a 110 l foam generating tank. The diluted, pressurized foaming agent was then mixed with compressed air flowing at 14 l s^{-1} at 0.69 MPa in a mixing nozzle to produce the preformed foam which was added to the cement slurry. The density of the cement foam is controlled by the amount of preformed foam added to the mix.

The mass flow rate of preformed foam was calibrated by measuring the time it took to fill a known volume with the preformed foam and weighing it; the quantity of preformed foam added to the cement slurry could then be controlled by timing its flow. The preformed foam was mixed into the cement slurry using a Univex 28 l mechanical food mixer with batter beater mixing blades. After thorough mechanical mixing, the wet cement foam was cast into 76 mm diameter, 152 mm high cylinder and 51 mm × 51 mm × 203 mm beam moulds to produce compression and flexural test specimens. The specimens were cured at ambient room temperature in a moist environment (90% relative humidity) for 12 days and air dried for an additional 2 days before mechanical testing. This technique was used to make cement foams with nominal densities of 240, 320, 400, 480 and 720 kg m^{-3}; unfoamed cement specimens (ρ = 1680 kg m^{-3}), made without the foaming agent, were also made.

The density of the cement foams was reduced by increasing the amount of preformed foam added to the mix. As a result, the water content and the water: cement ratio of the cement foams varied between 0.6 and 0.91 (Table II). The effect of the water cement ratio on the mechanical properties of the fully dense cement was measured by repeating the mechanical tests, described below, on specimens of fully dense cement with water: cement ratios of 0.6–0.91.

2.2. Microstructural characterization

The microstructure of each foam was characterized using digital image analysis of scanning electron micrographs. Microscopy specimens (12 mm cubes) of each density of cement foam were sawn from the beams used for the modulus of rupture tests. Five specimens from each of two beams of the 240, 320 and 400 kg m^{-3} cement foams and three specimens from one beam of the 720 and 1680 kg m^{-3} density materials were photographed and analysed. Prior to microscopy, the surface of each cube was impregnated with polymethylmethacrylate (PMMA) resin, polished and gold coated. Micrographs were taken at roughly × 15

TABLE II Cement foam characterization

Density (kg m^{-3})	W/C	Fully dense properties			Large void porosity	Matrix relative density
		E_s (GPa)	MOR[a] (MPa)	σ_{fs}^b (MPa)		
230	0.91	4.00	0.93	6.09	0.615	0.49
275	0.91	4.00	0.93	6.09	0.56	0.50
355	0.80	5.79	0.93	6.09	0.45	0.51
470	0.72	5.93	0.93	6.09	0.30	0.52
655	0.66	6.34	0.93	6.09	0.06	0.54
1680	0.60	8.21	0.93	6.09	0	1.0

[a] The modulus of rupture listed in this column is the value measured on 51 mm × 51 mm × 152 mm beams.
[b] σ_{fs} is the modulus of rupture of the cell wall material, estimated using the Weibull size effect, as explained in the text.

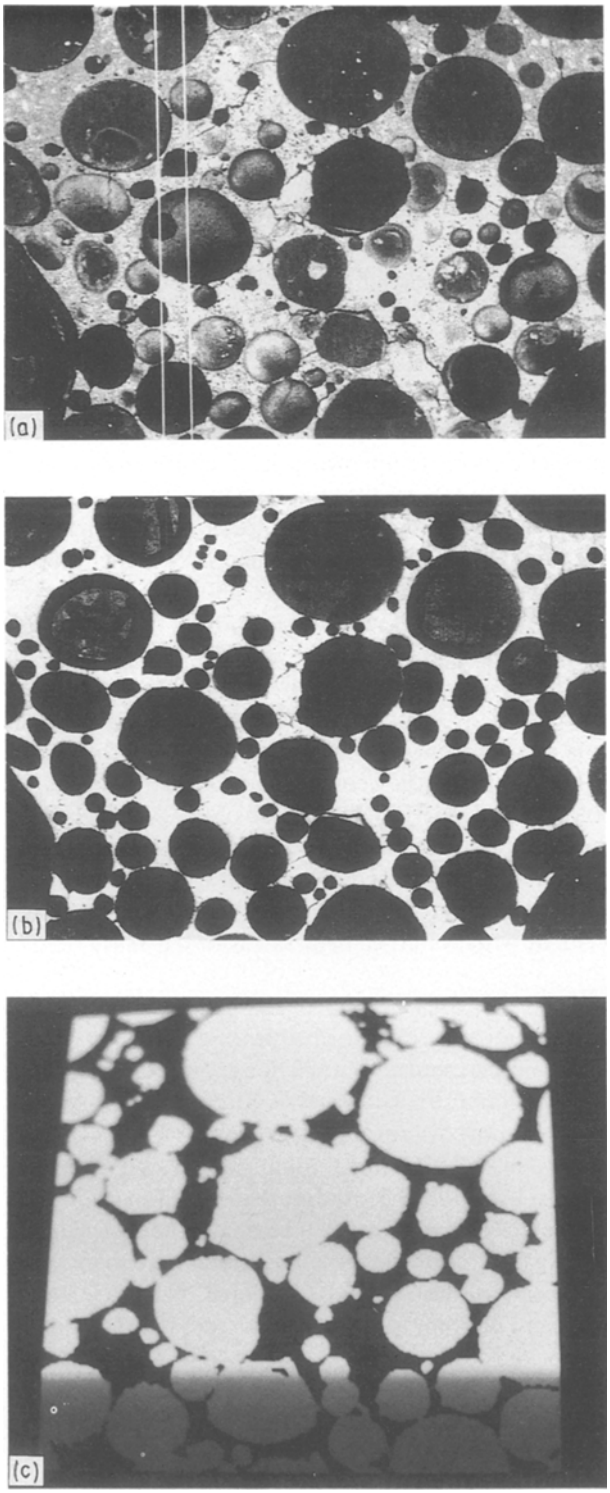

Figure 5 (a) Scanning electron micrograph of a cement foam specimen. (b) The same micrograph with enhanced contrast. (c) digital image of the micrograph with detected features shown in white.

to characterize large, coalesced voids and at $\times 40$ to characterize smaller, individual voids of the foam matrix. A single low-magnification micrograph was taken with the specimen centred in the viewing area; five higher magnification micrographs were taken to cover the same area.

The micrographs of the cement foam structure were digitized using a Magiscan 2 (Joyce Loebl, Newcastle, UK) image analyser, consisting of a video camera, an analogue to digital converter board and image processing software. To enhance the contrast on the micrographs before digitization, all voids were carefully darkened with a black marker. An original micrograph, the enhanced micrograph and the digitized image are compared in Fig. 5; the digitized image is a good representation of the original micrograph. The image analysis software was used to establish a size range for the detection of voids and to calculate the area of each void, the total area of all voids, the total frame area and the total area of all voids divided by the total frame area to give the porosity. Large, coalesced voids were found to have areas greater than 210 000 μm^2. Individual cells in the foam matrix were characterized by detecting voids with areas in the range 600–210 000 μm^2 on the higher magnification micrographs.

2.3. Mechanical testing

The Young's modulus, compressive strength and the modulus of rupture of each density of cement foam were measured. Cylindrical specimens (76 mm $\times$ 152 mm) were used for measuring Young's modulus and the compressive strength while the beams (51 mm $\times$ 51 mm $\times$ 203 mm) were used to measure the modulus of rupture. The cylinders were prepared for testing by trimming the ends and capping them with a rapid hardening, high-strength gypsum on a stand that ensured that the top and bottom caps were parallel to each other and perpendicular to the sides of the cylinder. The beams were prepared for testing by attaching two 13 mm $\times$ 13 mm $\times$ 76 mm mild steel pads to their bottom faces with gypsum at the support points.

The cylindrical specimens were tested in uniaxial compression (Fig. 6a); a 5000 N capacity, screw-driven materials testing machine (Instron Model 4201, Canton, MA) was used for testing the 240 and 320 kg m^{-3} cement foams, while a 270 kN capacity, hydraulic Baldwin machine with load ranges of 27, 107 and 270 kN, was used for testing the 480, 720 and 1680 kg m^{-3} materials. The Instron tests were done at a constant crosshead displacement rate of 0.5 mm min^{-1} while the Baldwin tests were done at rates of less than 1.5 mm min^{-1}. The specimens were centred in the loading platens and wax paper was placed between the specimen and the platens to reduce friction during testing. Two linear voltage displacement transducers were attached to the specimen using collars over a gauge length of 57 mm (Fig. 6b). In the tests done in the Instron, the load was measured directly from its load cell. In the tests done on the Baldwin, the pressure in the hydraulic line was measured using a pressure transducer, from which the applied load was calculated. The displacement output voltages from the two LVDTs and the load or pressure output voltages from the Instron or the Baldwin were recorded using a data acquisition system consisting of an IBM XT personal computer and Unkelscope software recording at a frequency of 2 Hz. The output of the data acquisition system was used to make load–displacement plots and to calculate the Young's modulus and the compressive strength of the specimens.

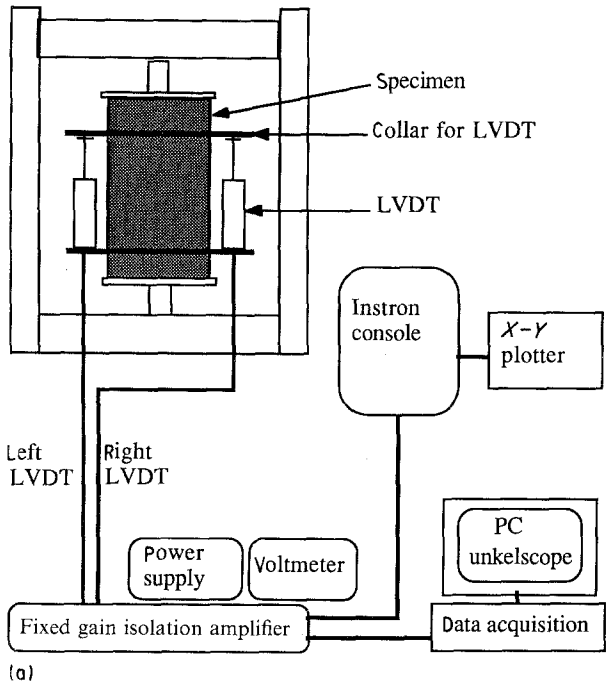

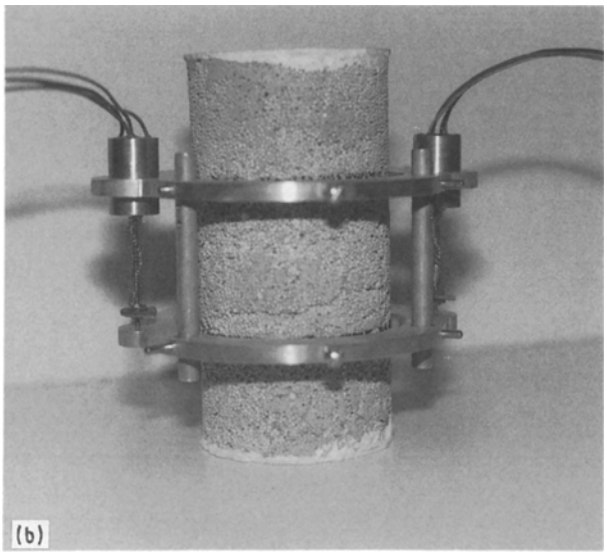

Figure 6 (a) Instrumentation for compression test for the measurement of Young's modulus and compressive strength. (b) Photograph of cement foam cylinder with transducers mounted.

The beam specimens were tested in three-point bending in the Instron testing machine, according to ASTM standard C 293–79 "Standard test method for flexural testing of concrete" (Fig. 7). The crosshead displacement rate was 1 mm min^{-1} in all of the tests. Load and crosshead displacement were recorded on an X–Y plotter; the maximum load applied was recorded from the Instron console.

In addition to the compression and bending tests on each density of cement foam, a limited series of tests were performed to measure the shear strength of the 400 kg m^{-3} cement foam. Sandwich beams with cement foam cores and stainless steel faces were tested in three-point bending to failure using the same setup as the modulus of rupture tests. The beams had a core thickness of 51 mm, a face thickness of 0.1 mm, a width of 51 mm, and a span of 152 mm. The load at

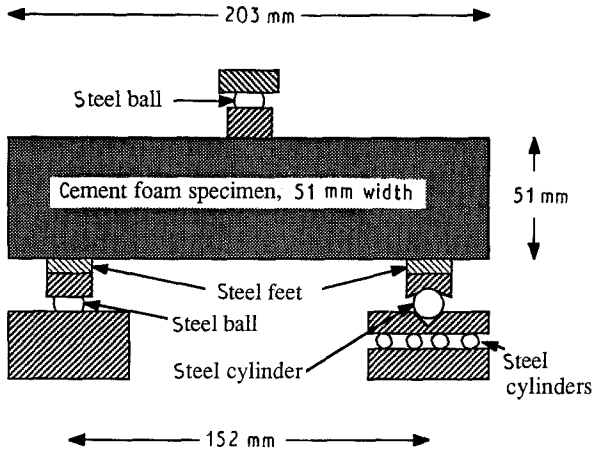

Figure 7 Schematic diagram of the three-point bending test for the measurement of the modulus of rupture.

which the core failed in shear was used to calculate the shear strength of the cement foam.

The effect of varying the water:cement ratio of the mix on the mechanical properties of the solid cement phase was determined by repeating the compression and bending tests on specimens of fully dense cement with water:cement ratios in the same range as those of the cement foams (W/C = 0.6–0.91).

3. Results

3.1. Microstructural characterization

Micrographs showing the microstructure of the 720, 400, 320 and 240 kg m^{-3} cement foams are shown in Fig. 1. The 720 kg m^{-3} cement foam has cells ranging in diameter from 20–500 μm with a median value of 210 μm. As the density of the cement foam is decreased below 720 kg m^{-3}, the stability of the foam decreases, causing individual cells to coalesce producing large voids. Image analysis of micrographs indicates that the coalesced voids have areas greater than 0.21 mm^2, corresponding to an equivalent diameter of 520 μm.

The volume fraction of the large coalesced voids and the relative density of the microporous foam matrix are listed in Table II. The relative density of the microporous foam is roughly constant at 0.5, while the volume fraction of large coalesced voids increases from 0.06 for the 655 kg m^{-3} foam to 0.615 for the 230 kg m^{-3} foam, suggesting that densities below 720 kg m^{-3} are achieved by the coalescence of individual cells into large voids within a foam matrix of roughly constant relative density.

3.2. Mechanical tests

A typical load–displacement plot for a compression test of the cement foam is shown in Fig. 2. The Young's modulus is calculated from the slope of the initial linear region of the plot while the compressive strength is calculated from the maximum load applied to the specimen. After the peak stress is reached, the specimen continues to carry about 60% of the peak stress up to relatively large strains; the test shown in the figure was discontinued after a strain of 2% was

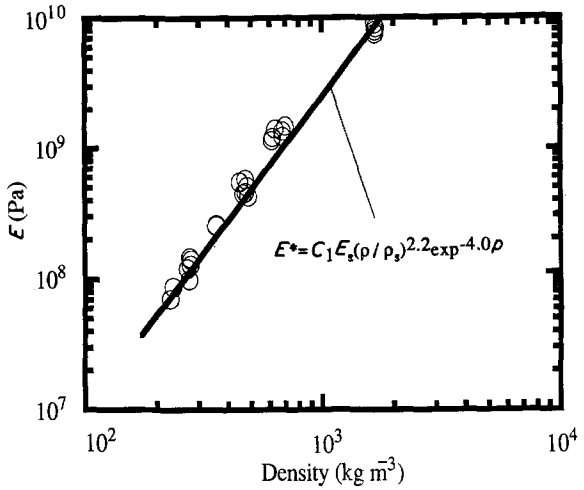

Figure 8 Young's modulus of cement foams plotted against density. (——) Equation (4) with $C_1 = 1$, $n = 2.2$ and $b = 4.0$.

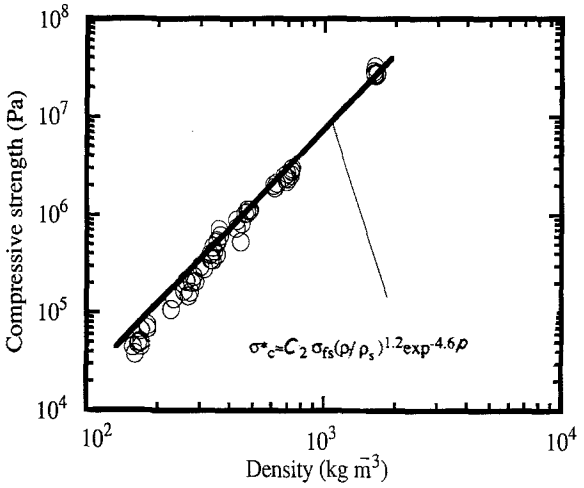

Figure 9 Compressive strength of cement foams plotted against density. (——) Equation (7) with $C_2 = 1$, $m = 1.2$ and $q = 4.6$.

reached. Young's modulus and compressive strength are plotted against density in Figs 8 and 9.

A load–displacement plot for a bending test on the cement foam is shown in Fig. 10. The modulus of rupture is calculated from the peak load, assuming a linear stress distribution across the section. The modulus of rupture is plotted against density in Fig. 11. The shear strength of the 430 kg m^{-3} cement foams averaged 0.145 MPa.

The effect of the water:cement ratio on the mechanical properties of the solid cement phase is listed in Table I.

4. Modelling

The microstructure of the cement foams can be modelled as large voids in a foam matrix (Fig. 12). The properties of the foam matrix are described by Gibson and Ashby's [6] model for closed cell foams. The presence of the voids is accounted for using empirical relationships for the mechanical properties of porous solids [7]; these relationships take the form $X = X_0\exp(-bp)$ where X and X_0 are the properties of

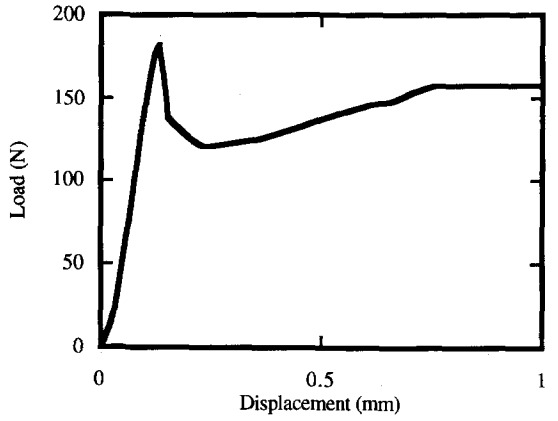

Figure 10 Load–displacement curve for 480 kg m^{-3} cement foam tested in three-point bending

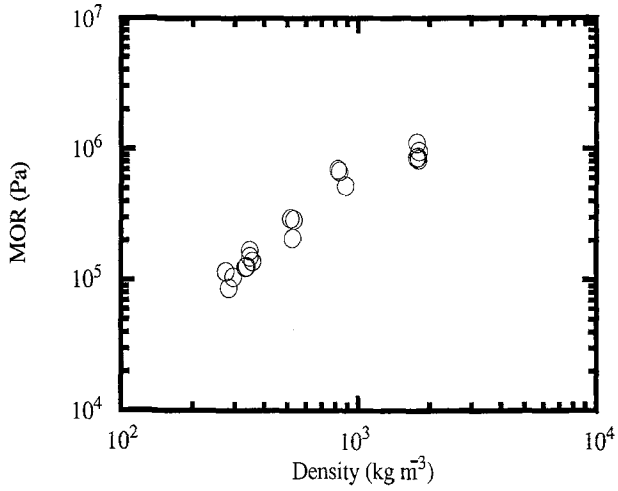

Figure 11 Modulus of rupture of cement foams plotted against density.

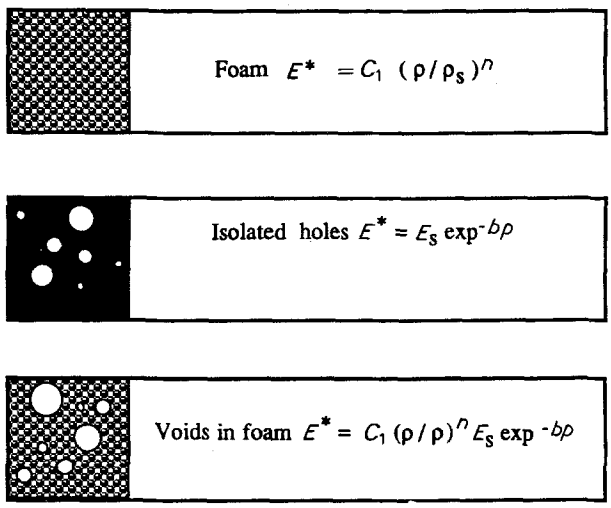

Figure 12 Schematic diagrams showing models for (a) a foam, (b) a porous ceramic (follows Rice [7]), and (c) voids in a foam. The equations next to each schematic give the corresponding relationship for Young's modulus.

the porous and fully dense solid, respectively, p is the porosity and b is an empirical constant.

Consider first the Young's modulus of the cement foams. The cell walls of a low-density closed-cell foam deform by plate bending if the plate deflections are

small compared to the plate thickness. Gibson and Ashby [6] have used dimensional arguments to show that the Young's modulus is then given by

$$E^* = C_1 E_s \left(\frac{\rho^*}{\rho_s}\right)^3 \quad (2)$$

where E^* and E_s are the moduli of the foam and the solid cell wall material, respectively, ρ^*/ρ_s is the relative density of the foam, and C is a constant. At relative densities greater than 0.3, axial and shear deformations also contribute to the modulus. The effect, which can be analysed exactly for a two-dimensional honeycomb-like structure [5, 8] is to reduce the exponent on the relative density from 3 to 2 at high densities. Because the relative density of the cement foam matrix is roughly 0.5, we expect the exponent to be between 2 and 3.

The effect of the large coalesced voids can be described by Rice's empirical equation [7]

$$E = E_0 \exp(-bp) \quad (3)$$

where E and E_0 are the Young's moduli of the porous and fully dense solids, p is the porosity and b is an empirical constant. Rice's review of data for ceramics with porosities up to 50% indicates that b varies from 1–11.5, with a mean value of 4. A semianalytical basis for deriving b has been developed by idealizing a ceramic as a granular material made of uniform spheres that coalesce together with different packing arrangements. By assuming that the strength was directly proportional to contact area, Knudsen [9] showed that $b = 6$ for closely packed spheres. Spriggs and co-workers [10–13] extended this concept to elastic properties and found similar values for b. Rice [14], reversing the roles of porosity and matrix, found $b = 3$ for high porosities ($p > 0.7$).

Combining the above results gives

$$E = C_1 E_s (\rho/\rho_s)^n \exp(-bp) \quad (4)$$

for a cement foam with large voids (of porosity p) in a foam matrix (of relative density ρ/ρ_s). We expect $n = 2$–3 and $b = 4$.

A similar approach can be taken for the compressive strength. The compressive strength of a brittle closed-cell foam in which failure occurs when the maximum tensile stress in the bent cell wall reaches the modulus of rupture for the wall material, is given by

$$\sigma^* = C_2 \sigma_{fs} (\rho^*/\rho_s)^2 \quad (5)$$

where σ^* and σ_{fs} are the compressive strength of the foam and the modulus of rupture of the cell wall material, respectively, and C_2 is another constant. Again, at high densities, the exponent is reduced by the contribution of axial and shear stresses in the cell wall; analysis of honeycombs suggests that it drops to a value of 1 at high densities.

The effect of the large coalesced voids can be described by Rice's equation for the compressive strength of a porous solid [7]

$$\sigma = \sigma_0 \exp(-qp) \quad (6)$$

where σ and σ_0 are the compressive strengths of the porous and fully dense solids, respectively. Rice notes that there is a wide range of values reported for the constant q; the average value is 7. Two studies have fitted equation 6 to porous cements. Verbeck and Helmuth [15] found $q = 1.3$ for cements with porosities from 9–40% while Rice [7] and Roy and Gouda [16] quote a value of $q = 6$ for cements with porosities between 0 and 20%. Semianalytical derivations suggest that for low porosities ($p < 0.45$) $q = 6$ [9] while for high porosities ($p > 0.7$) $q = 3$ [14].

Combining these results gives, for the cement foam with large coalesced voids

$$\sigma_c^* = C_2 \sigma_{fs} (\rho/\rho_s)^m \exp(-qp) \quad (7)$$

We expect the exponent m to have a value between 1 and 2 and the constant q to be about 3.

The modulus of rupture and the shear strength of cement foams depends on the fracture toughness and the size of the largest crack in the specimen; no attempt has been made to model either of these properties here.

5. Discussion

Fig. 8 shows data for the Young's modulus of 240–720 kg m^{-3} cement foams and of fully dense cement. The analytical expression for the Young's modulus of the cement foams, Equation 4, depends on three parameters: the Young's modulus of the solid cell wall material, the relative density of the foam matrix and the volume fraction of large, coalesced voids in the microstructure. All three parameters are listed for each density of foam in Table II. For densities below 640 kg m^{-3}, the relative density of the foam matrix is roughly constant at 0.5 and the Young's modulus of the cement foam is largely controlled by the volume fraction of large coalesced voids. For densities above 640 kg m^{-3}, the volume fraction of large coalesced voids is small and the Young's modulus of the cement foam is controlled by the foam matrix relative density. The solid line superimposed on the figure represents Equation 4 with $C_1 = 1$, $n = 2.2$ and $b = 4$, in good agreement with the values suggested above.

Fig. 9 shows data for the compressive strength of 240–720 kg m^{-3} cement foams and of fully dense cement. The analytical expression for the compressive strength, Equation 7, depends on the modulus of rupture of the cell wall material. Data for the modulus of rupture (MOR) measured on 51 mm × 51 mm × 152 mm beams of fully dense cements at water:cement ratios between 0.60 and 0.91 are given in Table II; water:cement ratios in this range have little effect on the measured modulus of rupture. The micrographs indicated that the 0.4 W/C material has a matrix porosity of 1% or less while the 0.6 and 0.91 W/C materials have matrix porosities of 7.6% and 9.5%, respectively. The similar moduli of rupture of the fully dense cements at W/C ratios between 0.60 and 0.91 is attributed to their similar porosities. The porosity of the fully dense specimens was investigated by examining micrographs, taken at × 39.8 and × 48.8 magnifications. Pores greater than 20 μm diameter were considered to contribute to matrix porosity, to

be distinguished from capillary porosity in the hardened cement paste. In our case capillary porosity was considered to be porosity created by pores less than 20 μm in diameter. Microscopy done at higher magnification indicated that this capillary porosity was affected by the water:cement ratio, with fully dense cement with a ratio of 0.91 having more capillary porosity than material with a ratio of 0.6. The cell walls of the cement foams have a much lower volume than the beams on which the modulus of rupture was measured; the cell wall modulus of rupture, σ_{fs}, was estimated using the well-known size effect, first described by Weibull [17]

$$\frac{\sigma_1}{\sigma_2} = \left(\frac{V_2}{V_1}\right)^{1/m} \quad (8)$$

where σ_1 is the measured modulus of rupture of a beam of volume, V_1, and σ_2 and V_2 are the modulus of rupture and volume of the cell wall material. The Weibull modulus, m, was estimated from tensile strength data available in the literature [18]; we found $m = 10.5$, a value similar to those for engineering ceramics. The volume of a cell wall was estimated from micrographs to be roughly 0.001 mm^3. Substituting these values into Equation 8 gives the cell wall modulus of rupture, σ_{fs}, indicated in Table II.

The solid line superimposed on the figure represents Equation 7 using the values of σ_{fs}, the volume fraction of large coalesced voids and the relative density of the foam matrix listed in Table II, with $C_2 = 1$, $m = 1.2$ and $q = 4.6$, in good agreement with the expected values for m and q.

The modulus of rupture of the cement foams is lower than the compressive strength at all densities. At low densities, the modulus of rupture of a foam typically approaches the compressive strength, due to the fact that both tensile and compressive failure are caused by tensile failure of the bent cell walls. The large coalesced voids may act as cracks within the foam matrix, decreasing the modulus of rupture of the cement foams. No attempt has been made to analyse the fracture mechanics of this process; an analysis of the fracture toughness of cement foams is required.

6. Conclusions

Low-density cement foams may be processed in several ways. In this study we made cement foams with densities in the range 160–720 $kg\,m^{-3}$ by introducing a preformed foam into a cement slurry. Microstructural characterization indicated that densities below 720 $kg\,m^{-3}$ are achieved by the coalescence of individual cells into large voids within a foam matrix of roughly constant relative density. The measured moduli and compressive strength of the cement foams were described by combining Gibson and Ashby's model [6] for closed cell foams with Rice's [7] empirical equations for porous solids. The fracture toughness of cement foams remains to be analysed.

The models presented indicate that with reductions in the water:cement ratio and void coalescence, very low-density (less than 240 $kg\,m^{-3}$) non-autoclaved cement foam can provide a desirable combination of economy, incombustibility and stiffness for many civil engineering applications. Further research into more stable, durable foams and foaming agents and processes that need less water is required.

Acknowledgements

This project has benefitted from advice and support from a number of sources, for which we are grateful. Dr Jack Germaine, Professor Leon Glicksman and Mr Steven Rudolph, MIT, and Mr Ned Glysson and Mr Leo Legatski, Elastizell Corporation of America, provided useful technical advice. Maia Hansen, Boris Ivanovic, Warren King and Debbie Min provided assistance with specimen preparation and testing. Financial support for the project was provided by the Innovative Housing Construction Consortium at MIT: Alcan International, General Electric Plastics Division, Illinois Tool Works, Mobay Chemical Corporation, US Gypsum corporation, and Weyerhaeuser Corporation. Fellowship support for Dr Tonyan was provided by the Program in Advanced Construction Technology at MIT, sponsored by the Army Research Office.

References

1. W. H. TAYLOR, "The production, properties and uses of foamed concrete", *Precast Concrete* (1974).
2. A. SHORT and W. KINNIBURGH, "Lightweight Concrete", 3rd Edn (Applied Science, London, 1978).
3. Misawa Homes Co. Ltd, "PALC Technical information" (Tokyo, 1988).
4. T. W. REICHARD, "Mechnical properties of insulating concretes", in "Lightweight Concrete", edited by D. P. Jenny and A. Litvin, (American Concrete Institute, Detroit, 1971) pp. 253–316.
5. T. D. TONYAN, PhD thesis, Department of Civil Engineering, Massachusetts Institute of Technology, Cambridge, MA (1991).
6. L. J. GIBSON and M. F. ASHBY, *Proc. Roy. Soc. Lond.* **A382** (1982) 43.
7. R. W. RICE, "Microstructural dependence of mechanical properties of ceramics", in "Treatise on Materials Science and Technology", Vol. II, edited by R. K. McCrone (Academic Press, New York, 1977) pp. 199–381.
8. GIBSON, L. J., PhD Thesis, Cambridge, UK (1981).
9. F. P. KNUDSEN, *J. Amer. Ceram. Soc.* **42** (1959) 376.
10. R. M. SPRIGGS, *ibid.* **45** (1962) 454.
11. R. M. SPRIGGS and L. A. BRISSETTE, *ibid.* **45** (1962) 198.
12. R. M. SPRIGGS, L. A. BRISSETTE and T. VASILOS, *ibid.* **45** (1962) 400.
13. R. M. SPRIGGS and T. VASILOS, *ibid.* **46** (1963) 224.
14. R. W. RICE, *ibid.* **59** (1976) 536.
15. G. J. VERBECK and R. A. HELMUTH, in "Proceedings of the Fifth International Symposium on the Chemistry of Cement", Vol. 3, Tokyo (1968) pp. 1–32.
16. D. M. ROY and G. R. GOUDA, *J. Amer. Ceram. Soc.* **56** (1973) 549.
17. W. WEIBULL, *Ing. Vetensk Akad. Proc.* **151** (1939) 1.
18. M. F. ASHBY and D. R. H. JONES, "*Engineering Materials*" **2** (Pergamon, Oxford, 1986).
19. L. J. GIBSON and M. F. ASHBY, "Cellular Solids: Structure and Properties" (Pergamon, Oxford, 1988).
20. L. M. LEGATSKI, "Significance of tests and properties of concrete and concrete making materials", ASTM Publication STP169B, ASTM Committee C-9 on Concrete and Aggregate (American Society for Testing and Materials, Philadelphia, PA, 1978).
21. R. W. RICE and B. K. SPERONELLO, *J. Amer. Ceram. Soc.* **59** (1976) 330.

Received 3 January
and accepted 4 February 1992